International Journal of Environmental Sciences
ISSN: 2229-7359
Vol. 11 No. 2s, 2025
https://www.theaspd.com/ijes.php

Spatial Estimation Of Gold (Au) And Copper (Cu) Using The Ordinary Kriging Method In The Judith Mining Concession, Napo

1st Soraya Bazurto Manzaba, 2nd Mayerly Plaza Cabrera, 3nd Joffre Andrade Candell & 4rd Fabián Peñarrieta Macias

Carrera de Ingeniería Ambiental. Escuela Superior Politécnica Agropecuaria de Manabí. Manuel Félix López, ESPAM-MFL, Campus Politécnico El Limón, vía Calceta-El Morro, Ecuador.

* *Corresponding author: soraya.bazurto@espam.edu.ec*

The expansion of metal mining into environmentally sensitive areas requires precise approaches to estimating the spatial distribution of minerals. This study applied geostatistical techniques to estimate the concentrations of gold (Au) and copper (Cu) in the Judith mining concession (265 ha), located in Napo, Ecuador. A total of 53 samples were systematically distributed (0.2 points/ha) and analyzed by inductively coupled plasma mass spectrometry (ICP-MS), ensuring analytical quality control. The spatial analysis used ordinary krigeado for Au and co-krigeado for Cu, integrating cross-validation in the SGeMS software. The results revealed a heterogeneous distribution: the Au presented maximum concentrations of 1.85 ppm, with a mean of 0.67 ppm and a median of 0.61 ppm in the northeast; Cu showed maximum values of 348.5 ppm, mean of 110.8 ppm and median of 109.4 ppm in the center-south. The models demonstrated a strong statistical fit (MSE: 0.013; MAE: 0.087 for Au), allowing the generation of thematic maps of spatial distribution. These estimates facilitated the delimitation of priority mineralized zones, improving extractive planning. It is concluded that geostatistics is effective in spatially projecting the concentration of Au and Cu, providing key inputs for the technical management of the resource, reduction of uncertainty and a more selective, strategic and environmentally controlled exploitation.

Keywords: *Environmental geochemistry, Special interpolation, Predictive modeling.*

INTRODUCTION

In 2019, 79% of theworld's production of metallic minerals was concentrated in five of the six biomes with the greatest global biodiversity. In particular, gold (Au) and copper (Cu) extraction has intensified in regions with severe water scarcity, raising significant environmental and social concerns (Luckeneder et al., 2021). In this context, geostatistics is consolidated as a key tool for the exploration and evaluation of deposits, by allowing a robust estimation of mineral concentrations and their spatial distribution (Mazari et al., 2023). Its application is crucial in mining concessions, as it facilitates more precise and profitable planning of exploitation, aligned with technical and environmental criteria (Zerzour et al., 2021).

In Ecuador, mining has acquired a leading role in economic development. In 2023 alone, the sector's exports reached USD 3,324 million, representing an increase of 19% compared to theprevious year (Verdezoto, 2023). This growth reaffirms the strategic relevance of mining in the country, but also shows the urgency of implementing sustainable management mechanisms that ensure a rational exploitation of resources, while mitigating their negative externalities (Mistler, 2022). The province of Napo, located in the

Ecuadorian Amazon, concentrates several extractive activities, including the Judith mining concession, located in the Carlos Julio Arosemena Tola parish and with an area of 265 hectares. This concession operates under the open-pit mining model, a technique that allows large volumes of material to be extracted with high efficiency, but which also implies a high environmental impact, particularly in soils and water bodies, due to the mobilization of heavy metals and toxic waste (Mestanza et al., 2022; Fan et al., 2022).

Added to this scenario is a growing expansion of illegal mining in Napo, a phenomenon that has escalated critically in the last two decades. This informal activity, characterized by the absence of environmental and regulatory controls, has led to the degradation of vast areas and the systematic contamination of sensitive ecosystems. Recent reports point to a 21% increase in areas affected by illegal mining in the province, which further aggravates the challenges for conservation and land use planning (Panchana, 2022; Mistler, 2022).

In this context, the incorporation of geostatistical techniques to estimate the spatial distribution of Au and Cu in the Judith concession is proposed as a high-value technical strategy. These methods make it possible to generate reliable predictive models that optimize the use of resources, while strengthening the scientific basis for implementing responsible mining practices (Afonseca and Costa, 2021). Geostatistics also facilitates the identification of critical areas that require specific environmental mitigation measures, contributing to a more comprehensive and sustainable management of the territory (Zerzour et al., 2021). Therefore, the objective of this research is to estimate the spatial concentration of Au and Cu in the Judith mining concession through the use of advanced geostatistical techniques. This estimation will make it possible to define mineralogical distribution patterns that guide efficient technical exploitation, minimizing ecological impacts and promoting a mining model aligned with the principles of sustainable development.

Method

The research was carried out in the Judith mining concession, located in the Carlos Julio Arosemena Tola parish, Napo province (Ecuador), with an area of 265 hectares. This area is geographically delimited by the UTM coordinates (Zone 17S), between the points East (X): 177,300 m and North (Y): 9,870,900 m. The predominant mining activity corresponds to the open-pit extraction system, which facilitates direct access to the surface layers of the substrate for geochemical sampling, without the need for deep drilling. A quantitative, exploratory and applied research design was adopted, with a geospatial and geostatistical approach. This design integrated spatial analysis techniques using Geographic Information Systems (GIS) and ordinary *kriging* interpolation methods , in order to model the spatial distribution of gold (Au) and copper (Cu) concentrations in the study area (Zerzour et al., 2021; Scott, 2022).

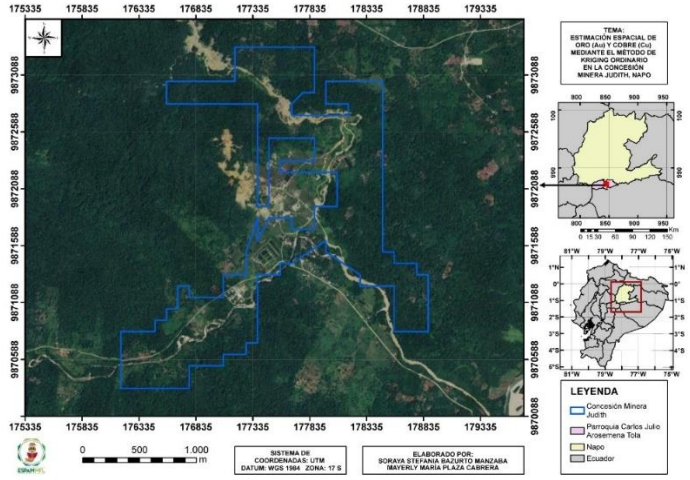

Figure 1. Geographical location of the study area.

Geospatial Data Collection

The field phase consisted of the systematic georeferencing of 53 sampling points distributed under a regular grid design, with an average density of 0.2 points per hectare, following mineralogical sampling standards (Lambert, 2016; Liang et al., 2021). The coordinates were recorded with a high-precision GPS (Garmin Montana 680), and subsequently corrected by positional error analysis in a GIS environment, contrasting with base topographic cartography and applying differential correction models (Niu et al., 2021). At each point, in addition to the location, morphological characteristics of the terrain, vegetation cover and lithological attributes were documented. This information was classified in situ according to morphostratigraphic and pedological criteria established for Andean-Amazonian terrains (Hannousse & Yahiouche, 2021).

SAMPLE SAMPLING AND TREATMENT

The sampling was aimed at capturing the horizontal and vertical variability of the deposit. Soil and rock samples were extracted at controlled depths of between 60 and 90 cm, using sterile hand holes and systematic sampling protocols to avoid cross-contamination. The samples were stored in sealed polyethylene bags, labeled with a unique code, and transported under stable thermal conditions to an ISO/IEC 17025 accredited laboratory (Dominy et al., 2021).

CHEMICAL ANALYSIS

The samples were subjected to complete acid digestion in HNO_3-HCl-HF matrix and subsequent quantitative determination by inductively coupled plasma mass spectrometry (ICP-MS), a technique that offers high sensitivity for trace metals (Giurlani et al., 2023). Analytical quality controls were incorporated through the use of targets, duplicates, internal standards, and certified reference materials (MRCs) in accordance with the QA/QC guidelines for geochemical explorations (Moles et al., 2013).

GEOSTATISTICAL ANALYSIS

The preliminary statistical analysis was performed in the SGeMS (Stanford Geostatistical Modeling Software) software, starting with an evaluation of normality, heteroskedasticity, and presence of *outliers*. Subsequently, omnidirectional experimental variograms were constructed, adjusted to Gaussian, exponential and spherical theoretical models. The selected model was the **Gaussian** model, as it had the lowest square error of fit and greater stability in spatial prediction (Arrieta et al., 2014).

Interpolation was executed by ordinary krigeado (OK) for both variables, using a tight Gaussian model and a search radius defined according to the spatial correlation range obtained in the variograms. Additionally, for the estimation of copper (Cu), ordinary co-krigeate was applied, incorporating gold (Au) as a secondary variable, given its more defined spatial structure and its usefulness as a geochemical guide in zones of associated mineralization (Patel et al., 2021). The validation of the model was carried out by means of *leave-one-out cross-validation*, using mean square error (MSE) and mean absolute error (MAE) as main metrics, defined as:

$$MSE = \frac{1}{n}\sum_{i=1}^{n}(\hat{Z}_i - Z_i)^2 \; ; \; MAE = \frac{1}{n}\sum_{i=1}^{n}(\hat{Z}_i - Z_i)^2$$

where $\hat{Z}_i$ is the estimated value and Z_i the observed value at location i.

GRAPHICAL REPRESENTATION OF SPATIAL DISTRIBUTION

As a result of the ordinary krigeado applied to the geochemical data, a raster representation of the spatial concentration of gold (Au) in the mining concession was generated, expressed on a continuous scale of colors. This map was obtained directly from the geostatistical processing environment, showing the areas of

greater and lesser accumulation of the metal. The values were coded using a chromatic scale ranging from blue (low concentrations) to red (high concentrations), allowing the areas of greatest mineralogical interest to be visually identified (Vaziri et al., 2021; Arrieta et al., 2014).

FINDINGS

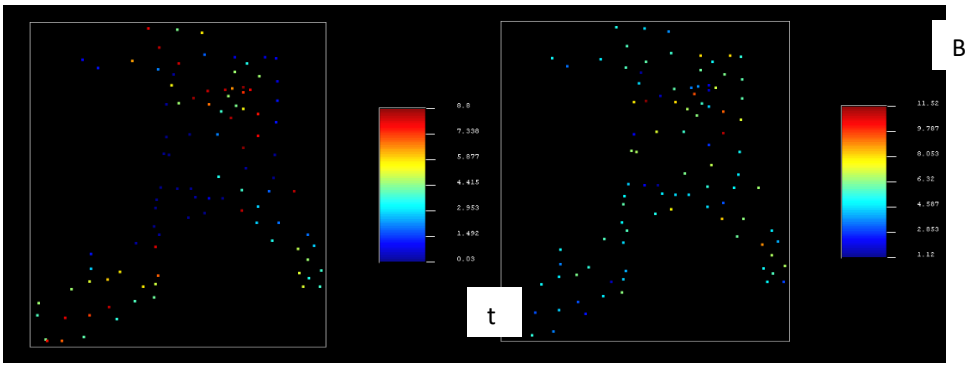

Figure 1. (a) Punto_Au and (b) Punto_Cu

Figure 2 shows well-defined clusters of high concentrations of both gold and copper, which coincide spatially with the nuclei of higher density estimated by ordinary kriging. This direct match between the raw data and the modelled values confirms the presence of mineralised zones with a coherent geochemical distribution and no artificial distortions. In the case of gold (Figure 2a), the high-grade points are concentrated towards the northeastern sector, while copper (Figure 2b) shows a more dispersed pattern, although with dominant foci in the central zone. The observed distribution not only supports the quality of the data collected, but also clearly delimits the most relevant metalliferous corridors of the evaluated area.

Statistical and Distributive Analysis

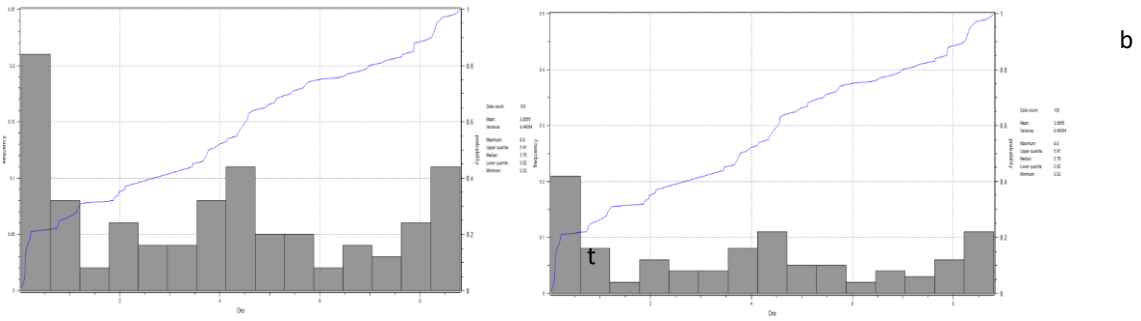

Figure 2. (a) Histograma_AuQ25 and (b) Histograma_AuQ50

The quartile histograms of gold (Figure 3 and Figure 4) clearly show a progressive enrichment dynamic in the deposit. In quartile 25 (Figure 3a), concentrations are mostly below 0.02 ppm, although point values close to 0.08 ppm are already emerging, revealing incipient zones of mineralization. This trend intensifies in quartile 50 (Figure 3b), where frequencies shift towards intermediate values (~0.04 ppm) and records above 0.1 ppm begin to consolidate, indicating a greater accumulation in localized sectors.

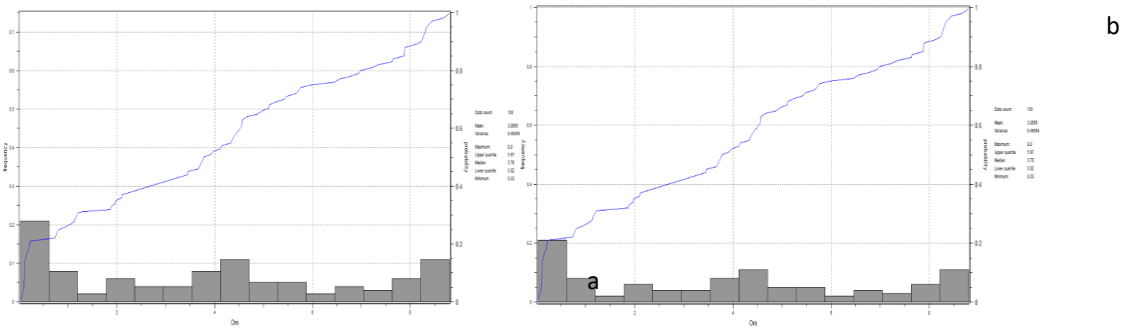

Figure 3. (a) Histograma_AuQ75 and (b) Histograma_AuQ100

In the upper quartiles, the gold behavior is even more defined. Quartile 75 (Figure 4a) reflects a substantial increase in concentrations, with recurrent values between 0.06 and 0.12 ppm and the appearance of outliers above 0.2 ppm. This statistical configuration confirms the continuity of the enrichment process in specific areas. In quartile 100 (Figure 4b), the histogram shows a marked asymmetry to the right, with values reaching up to 0.48 ppm. This bias reveals the presence of high-grade metalliferous cores, possibly linked to hydrothermal events or geological structures that favor gold concentration, consolidating the economic interest of the sector. In contrast, the geochemical behavior of Cu was less structured. The quartile histograms showed flat distributions without relevant accumulations, without registering extreme values or consistent trends. This homogeneous dispersion suggests a diffuse geochemical signal, lacking significant mineral concentration, which limits its exploitation potential under current conditions.

CORRELATION AND NORMALITY

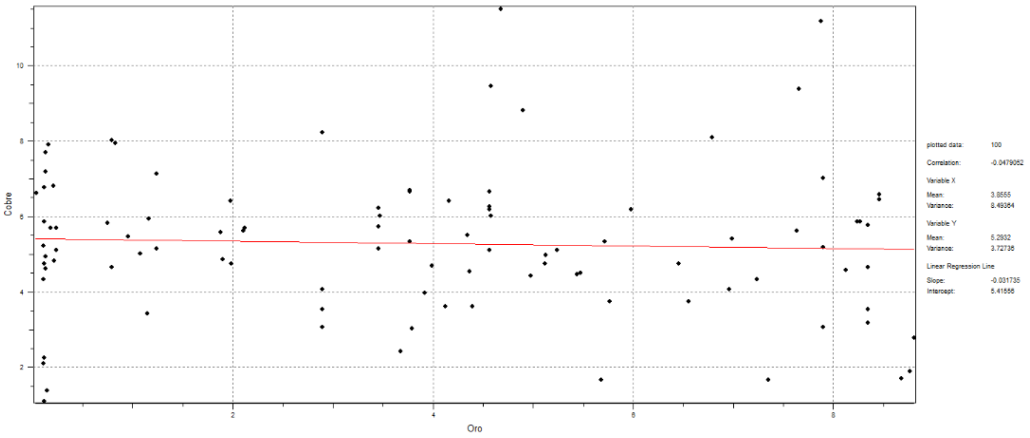

Figure 4. Scatterplot Au vs. Cu

The scatterplot between Au and Cu concentrations (Figure 5) reveals a weak to moderate positive relationship. Although an overall upward trend is identified, the point cloud is widely dispersed, limiting the statistical strength of the correlation. No anomalous clusters or cyclic structures were observed, suggesting a stable joint behavior. However, the presence of outliers in Au, higher than 0.60 g/t, introduces variability that could distort prediction models if not properly managed.

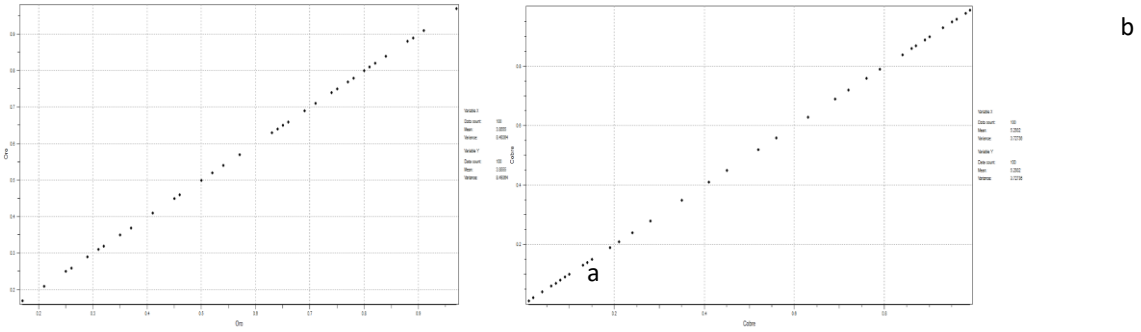

Figure 5. a) PP Plot – Gold and b) PP Plot – Copper

On the other hand, the PP graphs (Figure 6) confirm significant differences in the statistical distribution of both elements. In the case of Au (Figure 6a), there is a marked deviation from normal, especially at the extremes of the range (<0.10 and >0.60 g/t), reflecting a heterogeneous and biased distribution. This condition suggests the need to apply previous statistical transformations to any modeling that assumes normality. In contrast, Cu (Figure 6b) presented a much closer fit to the theoretical distribution, with more than 70 % of its values concentrated between 0.03 % and 0.07 %, which validates its suitability for geostatistical analysis without the need for prior adjustments.

Spatial Structure – Variograms

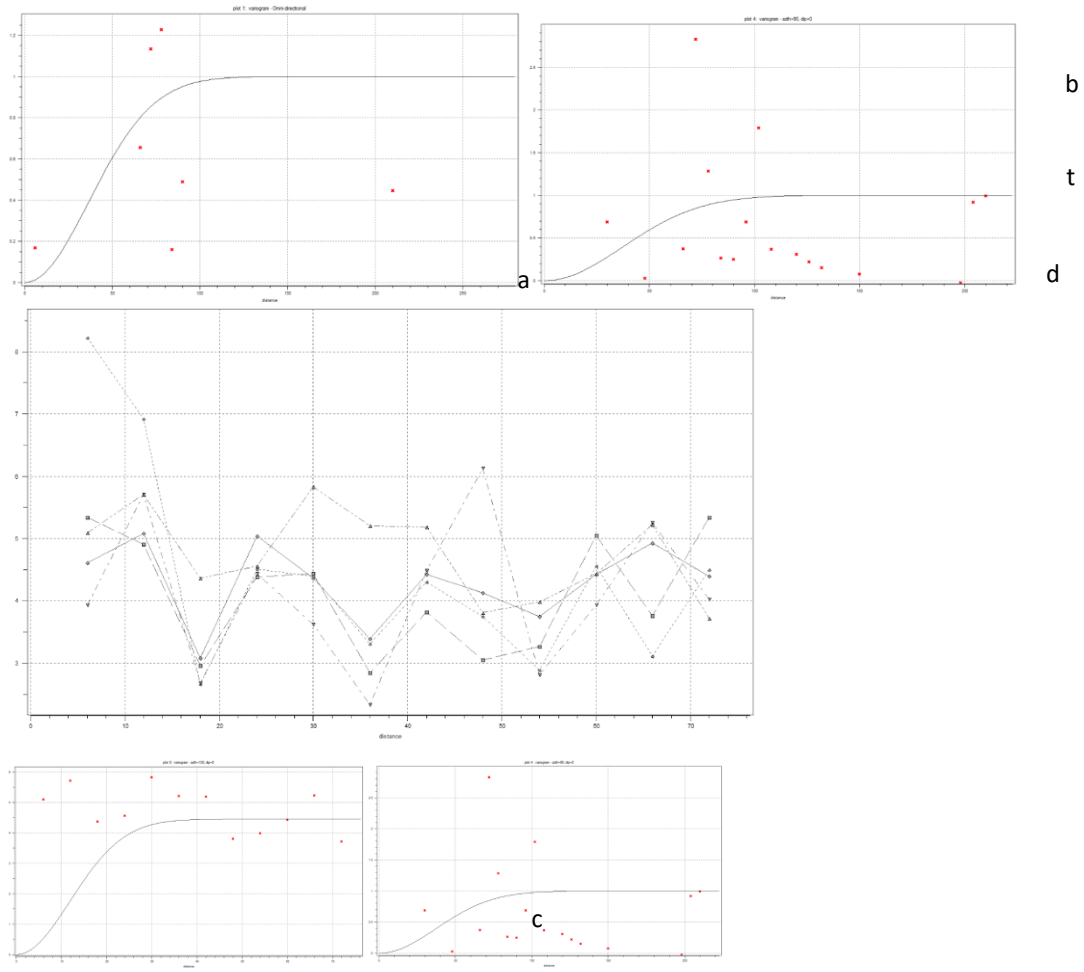

Figure 6. Cu and Au_azth variograms

The results derived from the variographic analysis showed contrasting spatial behaviors between **Cu** and **Au**, both in terms of continuity and direction. In the case of **Cu**, the omnidirectional variogram (Figure 7a) yielded a sill close to 0.25 and an effective range of approximately 100 meters. This configuration indicates a generalized spatial continuity without marked anisotropy, supported by a low nugget/sill ratio, confirming that most of the variability is structurally explained.

The 90° direction (Figure 7b) reinforced this pattern, with a slightly lower sill (~0.20) and a virtually negligible nugget (~0.02). The nugget/sill ratio of less than 10% evidences a highly marked local continuity, probably controlled by structural alignments such as veins or fractures parallel to that azimuth. This directionality reveals a defined and coherent spatial organization at the local scale.

In the 135° direction (Figure 7c), the growth of the Cu variogram was more gradual, with a sill that rose to ~0.30 and an extended range to 130 meters. This morphology suggests a regional structure of greater scope, possibly conditioned by oblique tectonic systems that define the mineralization in that orientation. In addition, the multidirectional model (Figure 7d) showed a smooth trend with sill of ~0.23 and a moderate nugget (~0.04), configuring a geochemical scenario with a controlled level of randomness (nugget/sill ~17%), useful for an integrated and balanced spatial representation.

In contrast, the spatial behavior of Au reflected greater heterogeneity. The 90° directional variogram (Figure 7e) showed a slightly higher sill (~0.28) and an extended range to 110 meters, signaling a longer continuity compared to Cu, and a greater total variability. This configuration suggests that the hydrothermal processes associated with gold mineralization have acted with greater dispersion and less structural control, which amplifies spatial heterogeneity.

Overall, the variographic models allow us to infer that Cu has a more stable and predictable structure at the local scale, while Au behaves with greater range, but also with greater dispersion. These differences directly condition estimation strategies: while Cu is more suitable for high-resolution local modeling, Au requires broader approaches, considering larger radii of influence and adjustments for heterogeneity. Both configurations, however, are technically sound for the application of kriging and, eventually, its extension to cokriging when it comes to integrating both variables

Spatial Estimation

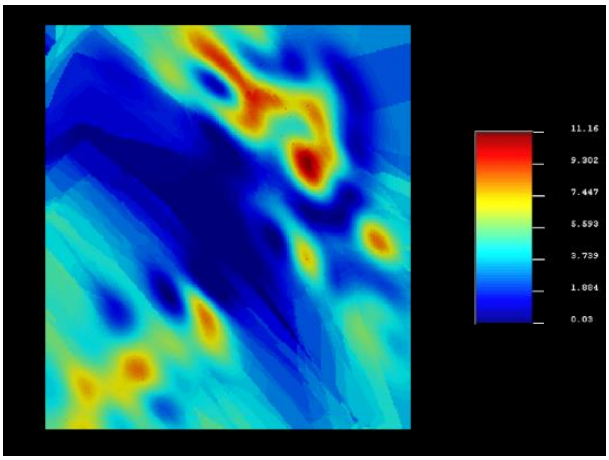

Figure 7. Mapa_KO_Au

The estimates obtained by ordinary kriging (KO) consolidated the spatial trends previously revealed by variographic analyses. In the case of Au, the estimated values fluctuated between 0.12 and 11.16 g/t, with a clear concentration of the highest grades in the northeast quadrant of the modeled block (Figure 8). This zone, defined by gold enrichment nuclei, remained consistent with the previously identified spatial

anisotropy directions, which reinforces the robustness of the model. Towards the southwest, concentrations decreased progressively, stabilizing below 1.0 g/t. This contrasting zoning suggests active structural control, possibly associated with vein systems or directed hydrothermal processes.

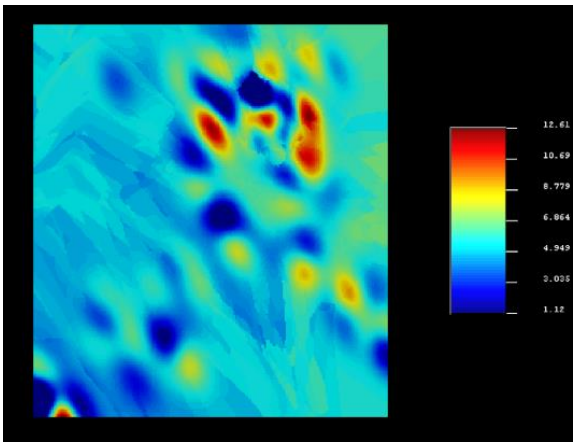

Figure 8. Mapa_KO_Cu

In the case of Cu, the estimates varied between 0.43 % and 12.61 %, with amore homogeneous spatial distribution (Figure 9). The highest values were located towards the north-central sector, although without a delimitation as marked as in the Au pattern. The transitions were smoother and the edges less defined, which can be attributed both to a lower density of primary data and to the influence of Au on the cokriging model used. Even so, areas with appreciable metal potential were identified, which justify more specific exploratory monitoring, particularly in areas of overlap with gold enrichment.

DISCUSSIONS

The progressive concentration of **Au** evidenced in the quartile histograms in the Judith mining concession, with values reaching up to 0.48 ppm, corresponds to the ranges reported by Arrieta et al. (2014), who when studying porphyry-type deposits in Andean contexts identified maximum grades of 0.45 ppm and a mean of 0.12 ppm. This coincidence suggests that the mineralization processes at Judith could be influenced by similar mechanisms, characterized by a gradual distribution of the metal in hydrothermal environments. On the other hand, the homogeneous distribution of **Cu** in Judith, without significant enrichments, contrasts with what was described by López (2016), who when analyzing the Recuay-Huaraz deposit reported an average of 0.949 % and maximum valuesof up to 3.447 %. This divergence may be associated with differences in structural and lithological controls, an aspect that Ouchchen et al. (2023) highlight as a determinant in the concentration of **Cu** in different geological systems.

The normality analysis carried out through PP graphs showed that the distribution of **Au** in Judith does not respond to normal behavior, presenting marked asymmetries at its ends. This condition was also reported by Navarro (2020) in the Condor project, where the correlation between **Au** and **Cu** was equally low, reflecting a limited mineralogical association between both elements. In Judith's case, the weak positive correlation between these metals supports that same dynamic, suggesting a likely independence in their concentration mechanisms. The marked asymmetry in the Au distribution, evidenced by the deviations in the PP graphs, is related to what was found by Díaz and Cuador (2019) in the Hierro Mantua deposit, who applied a logarithmic transformation to correct the skewed distribution of **Cu**, which reinforces the need to evaluate transformations when working with highly distorted variables. On the contrary, in Judith, the distribution of **Cu** is acceptably close to normal, which allows its direct modeling without resorting to transformations, thus facilitating the efficient application of geostatistical methods, as Koucham et al. (2024) warn when analyzing cases with similar behaviors.

The directional variograms constructed for the Judith deposit reveal definite spatial anisotropies, with effective ranges of up to 130 m for **Cu** and 110 m for **Au**. These magnitudes are within the expected values for mineralized systems in the Andes, as pointed out by Hammarstrom (2022), who documents a significant increase in **Cu** resources in that region, from 590 Mt in 2005 to 1600 Mt, in part due to the recognition of large and continuous spatial structures. The low nugget/sill ratio obtained in Judith, less than 10%, shows a high spatial continuity in both variables, an aspect that was alsoreported by Lytman et al. (2020) in the study carried out in Tintaya, where a strong spatial dependence of geomechanical properties was identified. This degree of continuity supports the applicability of the Kriging models used in Judith, by allowing a robust and reliable estimation of the laws of **Au** and **Cu** in the domain evaluated.

Au estimates obtained through Ordinary Kriging in the Judith mining concession reached maximum values of 11.16 g/t, significantly exceeding the average grades reported by Navarro (2020) in the Condor project, where 4.56 g/t were recorded. This difference suggests greater economic potential in Judith, at least in terms of the localized presence of high-grade areas. In the case of **Cu**, the application of Co-Kriging using **Au** as a secondary variable allowed to improve the accuracy of the estimates. This approach has been validated in research such as that of Du et al. (2021), who documented how Escudero and Morera optimized the Kriging plan through cross-validation, achieving a substantial improvement in resource estimation. The implementation of this type of methodologies in Judith contributes to reinforce the reliability of the geostatistical model applied, aligning it with modern practices in mineral evaluation.

While Ordinary Kriging has proven to be effective in estimating resources in Judith, emerging alternatives with operational and predictive advantages have been proposed in recent years. Christianson et al. (2022) highlight the use of Gaussian Processes as a tool that automates variogram inference and allows for better quantification of spatial uncertainty. For their part, Kirkwood et al. (2020) and Wang et al. (2021) applied Bayesian deep learning models to map geochemical variables from auxiliary information, achieving improvements in the accuracy of predictions compared to conventional methods. Although these techniques imply a greater computational demand, their future application could complement and enhance the results obtained by Kriging in complex exploratory scenarios such as Judith's.

CONCLUSION

The geostatistical estimation developed in the Judith mining concession allowed to characterize the spatial distribution of Au with technical rigor, identifying areas of high concentration with values that reach up to 11.16 g/t. This patternwas accompanied by a significant structural continuity, with an effective range of 110 m, and a marked spatial dependence evidenced by a nugget/sill ratio of less than 10 %. These indicators reflect a consistent mineralized system, technicallyrobust and with favorable projections in terms of economic viability. On the other hand, the geochemical distribution of **Cu**, although it did not show relevant enrichment patterns, was instrumental when used as a covariate in the Co-Kriging model, improving the resolution of the **Au** modeling by incorporating complementary spatial information. Together, the implementation of Ordinary Kriging and Co-Kriging not only proved to be methodologically sound and statistically valid, but also consolidated a reliable analytical platform for future stages of advanced exploration in the Judith field, opening opportunities to optimize the design of drilling campaigns based on spatial criteria.

REFERENCES

Afonseca, B. y Costa, J. (2021). Dynamic anisotropy and non-linear geostatistics supporting short term modelling of structurally complex gold mineralization. *REM - International Engineering Journal*, *74*(2), 199–207. https://doi.org/10.1590/0370-44672020740034

Arrieta, R., Sánchez, R., & Londoño, L. (2014). Geostatistical analysis for the estimation of gold and copper in porphyry-type deposits. *USBMed Engineering*, *5*(2), 80–88. https://doi.org/10.21500/20275846.313

Christianson, R., Pollyea, R. y Gramacy, R. (2022). *Traditional kriging versus modern Gaussian processes for large-scale mining data* (No. arXiv:2207.10138). arXiv. https://doi.org/10.48550/arXiv.2207.10138
Díaz, A., & Cuador, J. Q. (2019). Complexities of resource estimation in Bechi-type reservoirs in the northwest of Pinar del Río, Cuba, using nonlinear geostatistics. *Earth Science Bulletin*, *45*, 26–33. https://doi.org/10.15446/rbct.n45.73383
Dominy, S., Platten, I., Glass, H., Purevgerel, S. y Cuffley, B. (2021). Determination of Gold Particle Characteristics for Sampling Protocol Optimisation. *Minerals*, *11*(10), 1109. https://doi.org/10.3390/min11101109
Du, Q., Li, G., Zhou, Y., Wu, G., Chai, M. y Li, F. (2021). Distribution Characterization Study of the Heavy Metals for a Mining Area of East Tianshan Mountain in Xinjiang Based on the Kriging Interpolation Method. *IOP Conference Series: Earth and Environmental Science*, *719*(4), 042063. https://doi.org/10.1088/1755-1315/719/4/042063
Fan, T., Pan, J., Wang, X., Wang, S. y Lu, A. (2022). Ecological Risk Assessment and Source Apportionment of Heavy Metals in the Soil of an Opencast Mine in Xinjiang. *International Journal of Environmental Research and Public Health*, *19*(23), 15522. https://doi.org/10.3390/ijerph192315522
Giurlani, W., Biffoli, F., Fei, L., Pizzetti, F., Bonechi, M., Fontanesi, C. y Innocenti, M. (2023). Analytic procedure for the evaluation of copper intermetallic diffusion in electroplated gold coatings with energy dispersive X-ray microanalysis. *Analytica Chimica Acta*, *1269*, 341428. https://doi.org/10.1016/j.aca.2023.341428
Hammarstrom, J. (2022). Porphyry Copper: Revisiting Mineral Resource Assessment Predictions for the Andes. *Minerals*, *12*(7), 856. https://doi.org/10.3390/min12070856
Hannousse, A. y Yahiouche, S. (2021). Securing microservices and microservice architectures: A systematic mapping study. *Computer Science Review*, *41*, 100415. https://doi.org/10.1016/j.cosrev.2021.100415
Hodson, T. (2022). Root-mean-square error (RMSE) or mean absolute error (MAE): When to use them or not. *Geoscientific Model Development*, *15*(14), 5481–5487. https://doi.org/10.5194/gmd-15-5481-2022
Kirkwood, C., Economou, T. y Pugeault, N. (2020). *Bayesian deep learning for mapping via auxiliary information: A new era for geostatistics?* (No. arXiv:2008.07320). arXiv. https://doi.org/10.48550/arXiv.2008.07320
Koucham, M., Ait-Khouia, Y., Soulaimani, S., El-Adnani, M. y Khalil, A. (2024). 3D Geostatistical Modeling and Metallurgical Investigation of Cu in Tailings Deposit: Characterization and Assessment of Potential Resources. *Minerals*, *14*(9), 893. https://doi.org/10.3390/min14090893
Lambert, A. (2016). *Mineral Sampling* (p. 92) [Sampling Manual for Exploration, Underground Mining and Open Red]. Living geology. https://www.geologiaviva.info/wp-content/uploads/2021/07/Muestreo-de-Minerales.pdf
Liang, T., Werner, T. T., Heping, X., Jingsong, Y. y Zeming, S. (2021). A global-scale spatial assessment and geodatabase of mine areas. *Global and Planetary Change*, *204*, 103578. https://doi.org/10.1016/j.gloplacha.2021.103578
López, K. (2016). *Geostatistical procedure for the estimation of the copper concentration (in %) of the Recuay-Huaraz-Ancash mining deposit 2014* [To qualify for the provisional title of statistical engineer, National University of Trujillo]. https://dspace.unitru.edu.pe/server/api/core/bitstreams/92a8cbc4-3f5e-4ac5-95b0-a1d53d566f70/content
Luckeneder, S., Giljum, S., Schaffartzik, A., Maus, V. y Tost, M. (2021). Surge in global metal mining threatens vulnerable ecosystems. *Global Environmental Change*, *69*, 102303. https://doi.org/10.1016/j.gloenvcha.2021.102303
Lytman, S., Vargas, Z., Sánchez, V., & Tejada, L. (2020). *Correlation of the geotechnical indices (IS - UCS) with the lithology and alterations in Tintaya*. *2*(3), 8.

Mazari, M., Chabou, S., Bali, A., Kouider, K., Benselhoub, A. y Bellucci, S. (2023). Mineral resource assessment through geostatistical analysis in a phosphate deposit. *Naukovyi Visnyk Natsionalnoho Hirnychoho Universytetu*, *5*, 141–147. https://doi.org/10.33271/nvngu/2023-5/141

Mestanza, C., Cuenca, J., D'Orio, G., Flores, J., Segovia, S., Bonilla, A. y Straface, S. (2022). Gold Mining in the Amazon Region of Ecuador: History and a Review of Its Socio-Environmental Impacts. *Land*, *11*(2), 221. https://doi.org/10.3390/land11020221

Mistler, S. (2022). *InSight Crime–Investigation and Analysis of Organized Crime* [Journal]. InSight Crime - Investigation and Analysis of Organized Crime. https://insightcrime.org/

Moles, N., Chapman, R. y Warner, R. (2013). The significance of copper concentrations in natural gold alloy for reconnaissance exploration and understanding gold-depositing hydrothermal systems. *Geochemistry: Exploration, Environment, Analysis*, *13*(2), 115–130. https://doi.org/10.1144/geochem2011-114

Navarro, G. (2020). *Comparison between the application of Kriging and Cokriging to estimate copper species in a porphyry copper deposit* [Report to apply for the title of civil mining engineer, University of Chile]. https://repositorio.uchile.cl/bitstream/handle/2250/178050/Comparacion-entre-la-aplicacion-de-Kriging-y-Cokriging-para-estimar-especies-de-cobre.pdf?sequence=1

Niu, P., Cheng, Q., Liu, Z. y Chu, H. (2021). A machining accuracy improvement approach for a horizontal machining center based on analysis of geometric error characteristics. *The International Journal of Advanced Manufacturing Technology*, *112*(9–10), 2873–2887. https://doi.org/10.1007/s00170-020-06565-3

Ouchchen, M., Abia, E. H., Soulaimani, A., Abioui, M., Lutz, B., Benssaou, M., Abdelrahman, K., Abu-Alam, T., Echogdali, F. Z. y Boutaleb, S. (2023). The Missing Link in the Genesis of the Lower Paleozoic Copper Deposits of the Anti-Atlas (Morocco): The Late Triassic Central Atlantic Magmatic Province Event. *Minerals*, *13*(4), 488. https://doi.org/10.3390/min13040488

Panchana, A. (2022). *Illegal gold mining 'mafias' threaten life in an Ecuadorian river* [Journal Pollution]. Dialogue Earth | Global climate and environment news. https://dialogue.earth/en/

Patel, S., Solanki, C., Reddy, K. R. y Shukla, S. (Eds.). (2021). *Proceedings of the Indian Geotechnical Conference 2019: IGC-2019 Volume V* (Vol. 137). Springer Singapore. https://doi.org/10.1007/978-981-33-6466-0

Scott, T. J. (2022). *Preferred Leadership Style, Cognitive Operator Competencies, and Senior Leader Competencies Exhibited by United States Marine Corps Special Operations Officers: A Quantitative Non-Experimental Study*. *5*(2), 1447.

Vaziri, A., Nazarpour, A., Ghanavati, N., Babainejad, T. y Watts, M. (2021). An integrated approach for spatial distribution of potentially toxic elements (Cu, Pb and Zn) in topsoil. *Scientific Reports*, *11*(1), 7806. https://doi.org/10.1038/s41598-021-86937-1

Verdezoto, G. (2023). *Ecuador's Napo River is Dying. Again. New mining operations are killing all life in the Amazon tributary and impacting local communities* [Journal]. Earth Island Journal. https://www.earthisland.org/journal/index.php/

Zerzour, O., Gadri, L., Hadji, R., Mebrouk, F. y Hamed, Y. (2021). Geostatistics-Based Method for Irregular Mineral Resource Estimation, in Ouenza Iron Mine, Northeastern Algeria. *Geotechnical and Geological Engineering*, *39*(5), 3337–3346. https://doi.org/10.1007/s10706-021-01695-1